A&A 672, A136 (2023)
https://doi.org/10.1051/0004-6361/202245614

Astronomy & Astrophysics

Volatile exposures on the 67P/Churyumov-Gerasimenko nucleus*

S. Fornasier[1,2], H. V. Hoang[1,3], M. Fulle[4], E. Quirico[3], and M. Ciarniello[5]

[1] LESIA, Université Paris Cité, Observatoire de Paris, Université PSL, CNRS, Sorbonne Université, 5 place Jules Janssen, 92195 Meudon, France
e-mail: sonia.fornasier@obspm.fr
[2] Institut Universitaire de France (IUF), 1 rue Descartes, 75231 Paris, Cedex 05, France
[3] Université Grenoble Alpes, CNRS, Institut de Planétologie et Astrophysique de Grenoble (IPAG), UMR 5274, 38041 Grenoble, France
[4] INAF – Osservatorio Astronomico, Via Tiepolo 11, 34143 Trieste, Italy
[5] IAPS-INAF, via Fosso del Cavaliere 100, 00133 Roma, Italy

Received 2 December 2022 / Accepted 14 February 2023

ABSTRACT

Aims. We present the most extensive catalog of exposures of volatiles on the 67P/Churyumov-Gerasimenko nucleus generated from observations acquired with the Optical, Spectroscopic, and Infrared Remote Imaging System (OSIRIS) on board the Rosetta mission. We investigate the volatile exposure distribution across the nucleus, their size distribution, and their spectral slope evolution.
Methods. We analyzed medium- and high-resolution images acquired with the Narrow Angle Camera (NAC) of OSIRIS at several wavelengths in the 250–1000 nm range, investigating images from 109 different color sequences taken between August 2014 and September 2016, and covering spatial resolution from a few m px^{-1} to 0.1 m px^{-1}. To identify the icy bright spots, we adopted the following criteria: (i) they should be at least 50% brighter than the comet dark terrain; (ii) they should have neutral to moderate spectral slope values in the visible range (535–882 nm); (iii) they should be larger than 3 pixels.
Results. We identified more than 600 volatile exposures on the comet, and we analyzed them in a homogeneous way. Bright spots are found isolated on the nucleus or grouped in clusters, usually at the bottom of cliffs, and most of them are small, typically a few square meters or smaller. The isolated ones are observed in different types of morphological terrains, including smooth surfaces, on top of boulders, or close to irregular structures. Several of them are clearly correlated with the cometary activity, being the sources of jets or appearing after an activity event. We note a number of peculiar exposures of volatiles with negative spectral slope values in the high-resolution post-perihelion images, which we interpret as the presence of large ice grains (>1000 μm) or local frosts condensation. We observe a clear difference both in the spectral slope and in the area distributions of the bright spots pre- and post-perihelion, with these last having lower average spectral slope values and a smaller size, with a median surface of 0.7 m^2, even if the size difference is mainly due to the higher resolution achieved post-perihelion. The minimum duration of the bright spots shows three clusters: an area-independent cluster dominated by short-lifetime frosts; an area-independent cluster with lifetime of 0.5–2 days, probably associated with the seasonal fallout of dehydrated chunks; and an area-dependent cluster with lifetime longer than 2 days consistent with water-driven erosion of the nucleus.
Conclusions. Even if numerous bright spots are detected, the total surface of exposed water ice is less than 50 000 m^2, which is 0.1% of the total 67P nucleus surface. This confirms that the surface of comet 67P is dominated by refractory dark terrains, while exposed ice occupies only a tiny fraction. High spatial resolution is mandatory to identify ice on cometary nuclei surfaces. Moreover, the abundance of volatile exposures is six times less in the small lobe than in the big lobe, adding additional evidence to the hypothesis that comet 67P is composed of two distinct bodies. The fact that the majority of the bright spots identified have a surface lower than 1 m^2 supports a model in which water ice enriched blocks (WEBs) of 0.5–1 m size should be homogeneously distributed in the cometary nucleus embedded in a refractory matrix.

Key words. comets: individual: 67P/Churyumov-Gerasimenko – methods: data analysis – methods: observational – techniques: photometric

1. Introduction

Comet 67P/Churyumov-Gerasimenko (hereafter 67P) was the main target of the Rosetta mission of the European Space Agency. Launched in 2004, Rosetta took ten years to reach the comet before orbiting around it for ~25 months, from July 2014 to September 2016, permitting an in-depth investigation of the 67P nucleus morphology, physical properties, and composition, and of the cometary activity and the dust–gas interaction on the nucleus surface and the inner coma at different heliocentric distances. For the first time in space exploration Rosetta delivered a lander, Philae, on a cometary surface on 12 November 2014. Even if Philae rebounded from the original selected landing site, after an adventurous trajectory and a second rebound (O'Rourke et al. 2020), it reached the Abydos site where most of the foreseen in situ measurements were successfully achieved.

Rosetta revealed a complex morphology of the nucleus, with different kinds of terrains (Thomas et al. 2015), including layers, boulders, cliffs, and pits, sometime active (Vincent et al. 2015).

* Full Table A.1 is only available at the CDS via anonymous ftp to cdsarc.cds.unistra.fr (130.79.128.5) or via https://cdsarc.cds.unistra.fr/viz-bin/cat/J/A+A/672/A136

The cometary surface shows pervasive fractures ranging from millimeters (Bibring et al. 2015) to several tens of meters long produced by thermal insolation weathering (El-Maarry et al. 2015), as well as goosebumps or clod features on a scale of a few meters (Sierks et al. 2015; Davidsson et al. 2016; Fornasier et al. 2021) interpreted as remnants of the original pebbles or results of fracturing processes. Twenty-six regions, named after Egyptian deities, were identified based on the surface geomorphological properties (see El-Maarry et al. 2015, 2016 for the cometary regions definition and location). The bilobate shape of the nucleus, which shows extensive layering but with different centers of gravity between the large and small lobes, is associated with a binary structure resulting from the collision at low speed of two distinct bodies in the early Solar System (Massironi et al. 2015). The binary structure interpretation is also supported by the different mechanical and physical properties reported for the two lobes (El-Maarry et al. 2016; Fornasier et al. 2021).

The comet is dark with a geometric albedo of 6.5±0.2% at 649 nm (Fornasier et al. 2015). The nucleus composition is dominated by refractory material mixed with opaque minerals and organics. The spectrum is red (i.e., the reflectance increases in a steep way with the wavelength) and is characterized by a wide absorption band in the 2.8–3.6 µm region indicating the presence of a complex mixture of organics (Capaccioni et al. 2015; Quirico et al. 2016). The latest recalibration of the Visible, InfraRed, and Thermal Imaging Spectrometer (VIRTIS) gave evidence of different structures in the broad band, attributed to ammonium salts (Poch et al. 2020) and aliphatic organics (Raponi et al. 2020), with a possible contribution from hydroxylated amorphous silicates to the overall absorption (Mennella et al. 2020).

The nucleus shows compositional heterogeneities on several spatial scales, resulting in different spectral slopes and albedo in regional and local areas. On the dark and red average cometary terrain, exposures of volatiles stand out because they are very bright and with a bluer spectrum (i.e., less steep). Two volatile species were detected as exposed ice on comet 67P, mainly crystalline water ice (De Sanctis et al. 2015; Barucci et al. 2016; Filacchione et al. 2016a) and also carbon dioxide, the latter found for the very first time exposed at a comet surface (Filacchione et al. 2016b).

Joint observations of the Optical, Spectroscopic, and Infrared Remote Imaging System (OSIRIS) and VIRTIS spectrometers have proven that the bright and spectrally bluer features observed with the cameras display the typical water ice bands in the infrared spectra. Based on this correlation, a number of bluer and bright features detected with OSIRIS have been attributed to exposure of water ice (Barucci et al. 2016). Pommerol et al. (2015) reported the first OSIRIS detection of volatile exposures on comet 67P with features being 5–10 times brighter than the cometary dark terrain. Deshapriya et al. (2018) generated the first catalog of volatile exposures including 57 entries. Other studies highlight the presence of bright spots associated with water ice exposures in the northern hemisphere (Pommerol et al. 2015; Fornasier et al. 2015; Raponi et al. 2016; Barucci et al. 2016; Filacchione et al. 2016a; Lucchetti et al. 2017; La Forgia et al. 2015; De Sanctis et al. 2015; Oklay et al. 2017) and in the southern hemisphere (Fornasier et al. 2016, 2019a, 2021; Deshapriya et al. 2016, 2018; Hasselmann et al. 2019; Hoang et al. 2020), sometimes freshly exposed on the surface after cliff collapses or outbursts (Pajola et al. 2017a; Agarwal et al. 2017; Filacchione et al. 2016a) or due to the mechanical action of Philae (O'Rourke et al. 2020).

The estimated water ice abundance varies from a few percent (Barucci et al. 2016; Filacchione et al. 2016a,b; Raponi et al. 2016; De Sanctis et al. 2015; Ciarniello et al. 2016) to more than 20–30% in several bright areas observed in the Imhotep, Seth, Khonsu, Bes, Anhur, and Wosret regions (Deshapriya et al. 2016, 2018; Oklay et al. 2017; Pajola et al. 2017a; Fornasier et al. 2016, 2017, 2019a, 2021; Hasselmann et al. 2019; Hoang et al. 2020), with peaks up to ~50–80% in few localized tiny bright spots (Oklay et al. 2017; Hoang et al. 2020; O'Rourke et al. 2020; Fornasier et al. 2021), indicating fresh exposures of volatiles.

In this paper we present the most extended catalog of exposures of volatiles of comet 67P built upon a systematic analysis of the color sequences acquired with the OSIRIS cameras. We investigate their distribution in the different cometary regions and morphological terrains, their spectral slope evolution, their size distribution, and their duration with the aim of understanding volatile properties in comets, and of constraining cometary models.

2. Observations and methodology

The analysis is based on data from the OSIRIS imaging system of the Rosetta mission. OSIRIS included two cameras, the Narrow Angle Camera (NAC) for the high-resolution study of the nucleus, and the Wide Angle Camera (WAC) for the coma investigation (Keller et al. 2007).

We analyzed medium- and high-resolution images acquired with the NAC camera with several filters in the 250–1000 nm range, investigating 109 different color sequences taken between August 2014 and September 2016, and covering a spatial resolution from a few $\mathrm{m\,px^{-1}}$ up to $0.1\,\mathrm{m\,px^{-1}}$. We searched in the OSIRIS archive all the NAC spectrophotometric sequences pointing to the 67P nucleus and having at least three filters. Exposures of volatiles are usually brighter than the comet dark terrain, and are characterized by a neutral to moderate spectral slope in the visible range, which has been proven to be associated with a local enrichment in water ice thanks to joint observations carried out with the OSIRIS cameras and the VIRTIS spectrometer (Barucci et al. 2016; Filacchione et al. 2016a). Thus, to determine whether a bright feature on the surface is ice dominated and not simply brighter because of illumination conditions, information on the reflectance value and on the spectral slope of a region of interest (ROI) are needed. This implies that some bright spots observed only in the NAC orange filter centered at 649 nm, the filter most frequently used to generate the nucleus shape model or to investigate the comet morphology, are not included in our analysis. With only one filter available we cannot determine if the higher brightness is due to a geometric effect, to the presence of a bright mineral, or to a real exposure of ice.

Therefore, we applied the following methodology to identify exposures of volatiles on the 67P nucleus. Bright spots exposing volatiles should be both brighter (by at least 50%) than the comet dark terrain, and should have neutral to moderate spectral slope values in the visible range (535–882 nm). The adopted upper limit in the spectral slope value is 11%/(100 nm), but usually bright spots have spectral slopes much lower than 8%/(100 nm), and often close to zero. Moreover, we considered only the bright spots larger than 3 pixels. Smaller features are indeed difficult to characterize because of residuals in the images co-registration process.

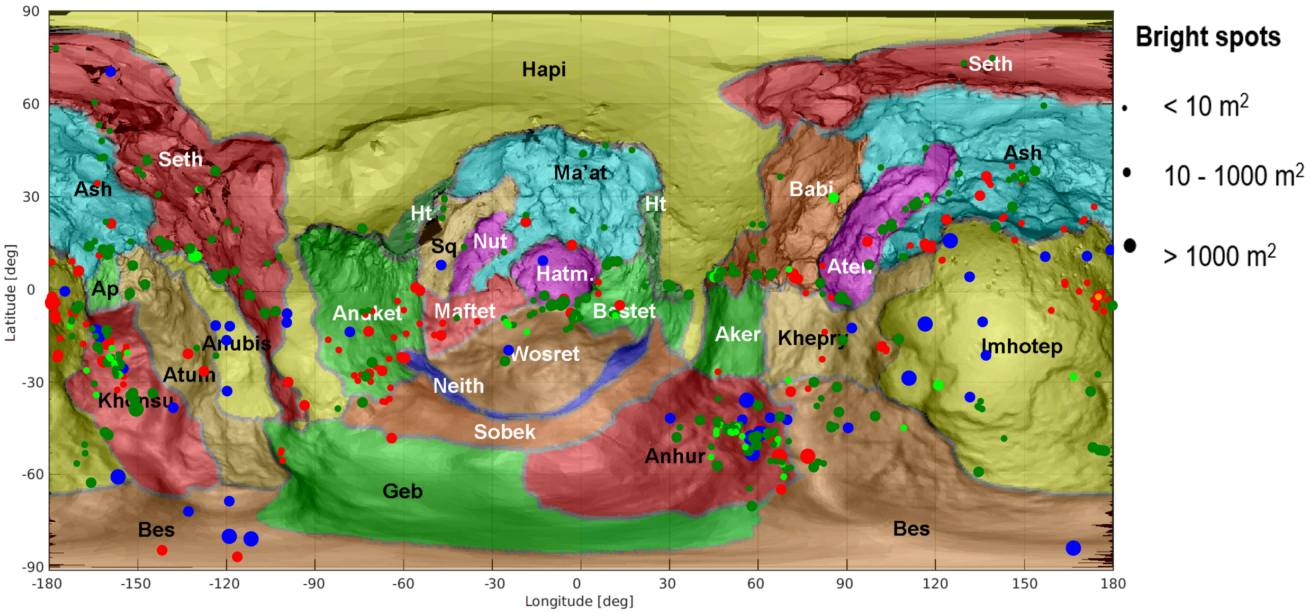

Fig. 1. Maps of ice exposure on comet 67P. The color-coding is as follows: red, pre-perihelion (August 2014–May 2015); cyan, perihelion (June–October 2015); green, post-perihelion (November 2015–September 2016). The spectrally blue spots, those having negative spectral slope (<−3%/(100 nm)) in the 535–882 nm range, are shown in light green (post-perihelion) and orange (pre-perihelion). The symbol size represents three ranges of volatile exposure area; they are not in scale compared to the nucleus surface (51.74 km^2 in total; Thomas et al. 2018), but are enlarged for clarity.

We used the NAC images generated by the instrument pipeline (Tubiana et al. 2015) corrected by bias, flat field, geometric distortion, absolutely calibrated in radiance, and finally converted in radiance factor (also named I/F)

$$\text{Radiancefactor}\,(i,e,\alpha,\lambda) = \frac{\pi I(i,e,\alpha,\lambda)}{F sun_\lambda}, \quad (1)$$

where I is the scattered radiance at a given incidence (i), emission (e), phase (α) angles and wavelength (λ), and $F sun_\lambda$ is the incoming irradiance of the Sun at the heliocentric distance of the comet and at a given wavelength (λ).

As done in previous studies of the 67P nucleus, the NAC images of a given sequence were first co-registered using the F22 NAC filter (centered at 649.2 nm) as a reference, then corrected by the illumination conditions using the Lommel–Seeliger disk function and the 3D stereophotoclinometric shape model of the 67P nucleus (Jorda et al. 2016), adopting the same methodology already presented in Hasselmann et al. (2019) and Fornasier et al. (2017, 2019a).

We also created RGB images with the STIFF software, which converts scientific FITS images to TIFF (Bertin 2012), mostly using the filters centered at 882 nm (R), 649 nm (G), and 480 nm (B). These RGB images are very helpful in identifying volatile exposures since they look bright and blue compared to the dark and red cometary terrain.

For each bright feature, the spectral slope ($S\,l$) was computed in the 535–882 nm range as:

$$S\,l = \frac{R_{882} - R_{535}}{R_{535} \times (882\ \text{nm} - 535\ \text{nm})}, \quad (2)$$

where R_{882} and R_{535} are the radiance factors in the filters centered at 882 nm and 535 nm, respectively.
Details on the observing conditions are reported in Table A.1.

3. Catalog of volatiles exposures

We identified and characterized 603 bright spots (hereafter BS) having a spectral slope much lower than the typical value of the cometary dark terrain (Table A.1), thus indicating local exposures of volatiles, very likely water ice on the 67P nucleus. This is the most complete catalog of volatile exposures on 67P published to date, increasing by a factor of ∼10 the number of identified bright spots on the comet compared to data already published in the literature. However, this catalog does not include the totality of the volatile exposures for the following reasons: (i) some BS might have been present on the surface but not captured by OSIRIS observations because Rosetta was pointing elsewhere or because they fully sublimated between two consecutive OSIRIS sequences covering a given region; (ii) in this catalog we included only the BS observed within color sequences, thus we do not consider those captured by a single filter where the spectrophotometric analysis cannot be performed; (iii) we considered only the bright spots larger than 3 pixels in size; (iv) in the case of clusters of icy exposure, not all the individual points (often smaller than 3 pixels in size) were counted.

For each bright feature we computed the surface, the coordinates, the spectral slope, and the minimum duration, when possible, and for a few showing negative spectral slope values we also estimated the water ice abundance using geographical mixtures of the comet dark terrain and water ice. The full catalog of bright spots is reported in Table A.1, and their distribution across the nucleus is shown in Fig. 1.

4. Bright feature distribution and type

Bright patches and spots could be found isolated on the nucleus surface or grouped in clusters, usually at the bottom of cliffs. In Tables 1 and A.1 we report the BS type following the

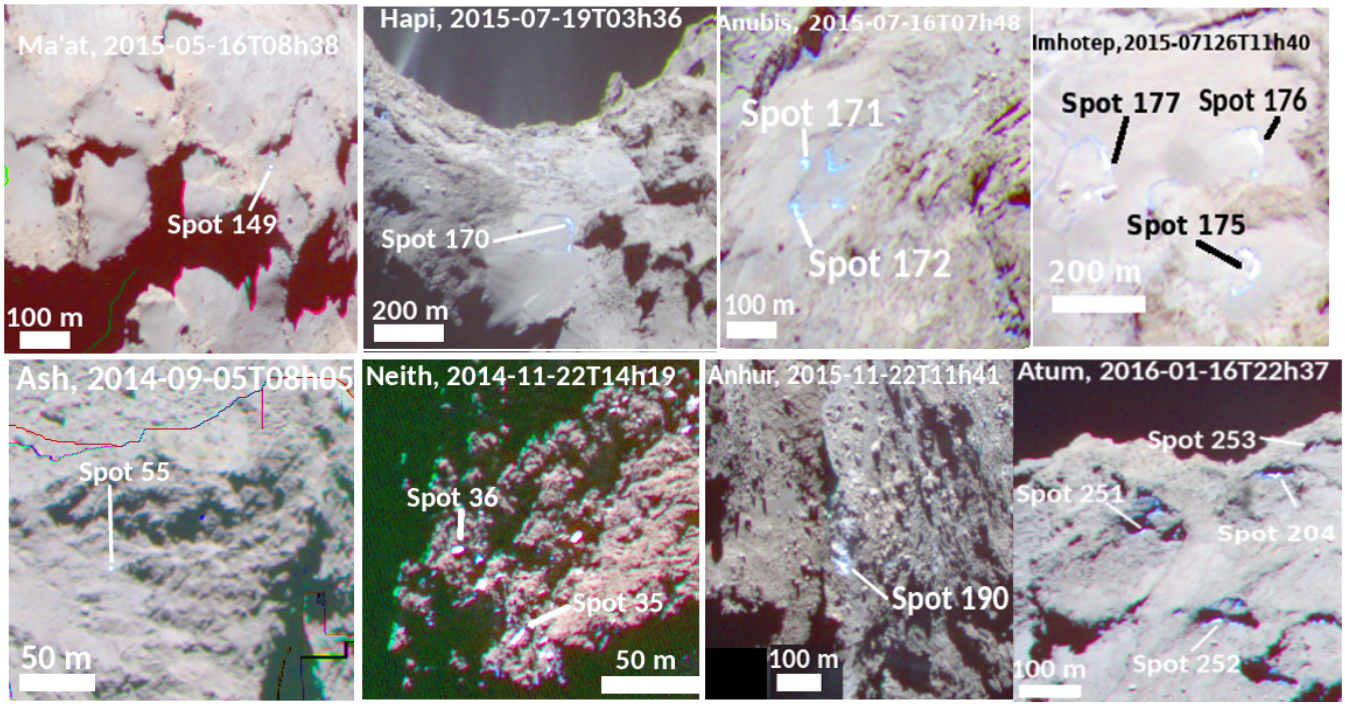

Fig. 2. Example of isolated bright features on smooth terrains (top) and close to irregular structures (bottom), feature types 1 and 2, respectively, following the Deshapriya et al. (2018) classification scheme. The bright spot numbers correspond to those listed in Table A.1.

Table 1. Volatile exposures types from the catalog here presented (Table A.1) following the Deshapriya et al. (2018) classification scheme.

Feature type	Number	< Area > (m^2)	< Duration > (days)
1 Isolated BS on smooth terrains	27	371	18.1
2 Isolated BS close to irregular structures	373	86	40.5
3 BS resting on boulders	58	24.5	71.6
4 Clusters of BS	145	23	35.9

Notes. BS=bright spots. The average area and duration are reported for each type.

Deshapriya et al. (2018) classification scheme: type (1) isolated BS on smooth terrains; type (2) isolated BS close to irregular structures; type (3) BS on top of boulders; type (4) clusters of bright patches and BS.

Examples of the different types of volatiles exposures are reported in Figs. 2–4, while in Table 1 we summarize the BS identification per type. The majority of them are of type 2, and are thus identified close to irregular structures. This is quite expected because of the complex geomorphology of the comet.

The largest icy exposure belongs to type 2 and was observed on Imhotep shortly after the perihelion passage, on 23 August 2015 (BS 188 in Table A.1). This bright patch occupied a vast surface of ~5260 m^2, and was repeatedly observed for 4 h by NAC sequences capturing that region, and was still observed one week later, even if part of it sublimated during this time lapse. It is worth mentioning that this area was brighter and spectrally bluer than the comet dark terrain, but its spectral slope was relatively high compared to other BS (around 10%/(100 nm)), indicating a local surface enrichment of volatiles, but highly mixed with the cometary dust. In addition, the spatial resolution was relatively low (about 6 m px^{-1}), impeding an accurate study of this BS.

More than one-third of the type 2 BS are smaller than 1 m^2, and the average size is of 86 m^2, or 72 m^2 when excluding the largest patch previously described. For 136 out of 373 BS of type 2, we estimated their minimum duration (i.e., the time between the first and last sequences capturing a BS), and its average value is 41 days.

Smooth terrains (type 1, Fig. 2) host few BS, but they tend to be larger (~370 m^2) than the isolated ones observed close to irregular structures or on boulders, and their average duration is the shortest (about 18 days, Table 1). This may be attributed to mixing processes with the surrounding dust, and/or to a longer illumination time and/or intensity compared to rough terrains where mutual shadows favor a longer ice survival.

Conversely, BS on boulders (type 3, Fig. 3) are found to be smaller in size but with the longest duration (72 days). This may be associated with the presence of fractures and small cavities on boulders, which slow down the volatile sublimation. Bright spots on boulders may also be fed by internal reservoirs of volatiles. During the second Philae touch down, the lander imprinted in a boulder, revealing a 3.5 m^2 bright area containing the primordial water ice embedded inside it (O'Rourke et al. 2020). They estimated a water ice fraction of 46% and a dust-to-ice mass ratio of 2.3 in this boulder.

Clusters of bright spots (type 4, Fig. 4) are located at the bases of cliffs and likely formed as a result of cliff collapses, such as the large clustered features (CFs) named CF1, CF2, and CF3 described in Oklay et al. (2017). Some of them, especially in post-perihelion images, look clearly associated with frost recondensation, like the ones in the Ash and Babi regions shown in Fig. 4. We identified 145 BS in clusters, located mainly in the Anuket, Ash, Aten, Babi, Geb, Hatmehit, and Seth regions. The individual BS in clusters are relatively small (23 m^2), and some